P1.13

USING QUIKSCAT-DERIVED SURFACE WINDS AND A GCM TO IMPROVE PREDICTED WIND SPEED VARIABILITY AND OCEAN SURFACE FLUXES

Scott B. Capps*
Dr. Charles S. Zender†
Univ. of California, Irvine, California

1. IMPORTANCE OF SUB-GRIDSCALE WINDS

Winds at the surface play a key role in climate processes by determining air-sea energy and gas exchanges. Although steady and continuous in some regions, these non-linear exchanges can be dominated by the tail of the wind speed distribution in regions and periods of strong wind variability. Such variability includes climatically extensive regions such as the Intertropical Convergence Zone (ITCZ) where convective downdrafts are common (Donelan et al., 2002), to propagating westerly wind bursts on intra-seasonal timescales (Weller and Anderson, 1996), to storm track gustiness. Surface heat and energy fluxes depend non-linearly on wind speed magnitude (Freely et al., 2004; Renfrew et al., 2002; Wang et al., 1998), are sensitive to the tails of the wind distribution, and hence vary significantly on spatio-temporal scales not resolved by GCMs. NASA QuikSCAT data offer the opportunity to characterize wind speed probability density functions (PDFs) across climatically significant spatial and temporal scales (e.g., Monahan, 2006a). I propose to use these data to improve understanding and prediction of fluxes from sub-gridscale winds, and thus improve atmosphere-ocean coupling in models contributing to the fifth IPCC assessment report.

The NASA QuikSCAT scatterometer dataset [1] provides six complete years (Jan./2000–Dec./2005) of accurate (Bourassa et al., 2003), twice-daily instantaneous ocean surface wind speed estimates (Chelton and Freilich, 2005) at $0.25^\circ \times 0.25^\circ$ resolution. The 2000–2005 climatological mean of four statistics of the surface wind speed PDFs computed from QuikSCAT measurements illustrates the global spatial variation of the mean wind speed $\bar{U}$, its temporal variability (shown as standard deviation σ), Weibull shape factor k (defined below), and maximum value $U_{\max}$ (Figure 1, row 1, columns 1–4, respectively). NCEP reanalysis which incorporate QuikSCAT and constraints from other data streams, are a second observationally-based estimate of global surface winds. Consistent with the relatively coarser (6-hourly vs. instantaneous) NCEP data, global oceanic regions are dominated by negative wind speed mean and maximum differences (Figure 1, second row).

1.1 Wind Speed Biases

Our level of understanding of global ocean surface wind speed variability is demonstrated, in part, by the biases between observed wind speeds and predictions of general circulation models (GCMs). The GCM we employ is the Community Atmosphere Model (CAM3) (Collins et al., 2006), the atmospheric component of the NCAR Community Climate System Model (CCSM). Simulations are performed at T85 resolution (approximately $1.4^\circ \times 1.4^\circ$ equatorial with 26 levels). Sub-sampling the CAM3 2000–2005 predictions (forced by observed sea surface temperatures (SSTs)) at QuikSCAT overflight times (0600 and 1800 local time) permits a direct intercomparison of QuikSCAT and CAM3 wind speed climatologies. Capps and Zender (2007) describe these climatologies in greater detail.

Significant biases between observed and modeled wind speed and wind speed variability occur from 2000–2005 (Figure 1, third row). Most of the $0.39\,\mathrm{m\,s^{-1}}$ global mean CAM wind speed bias occurs in the southern hemisphere (SH) circumpolar region, northern hemisphere storm tracks, and trade wind regions. Sizable swaths of biases $\sim 3.0\,\mathrm{m\,s^{-1}}$ occur along the SH storm track near Australia. CAM3 underestimates wind speeds in the ITCZ and along the western coasts of Africa,

*Scott B. Capps, Univ. of California, Irvine, Dept. of Earth System Science, Irvine, CA 92617; e-mail:scapps@uci.edu
†Dr. Charles S. Zender, Univ. of California, Irvine, Dept. of Earth System Science, Irvine, CA 92617; e-mail:zender@uci.edu

[1] http://podaac.jpl.nasa.gov:2031/DATASET_DOCS/qscat_L3.html

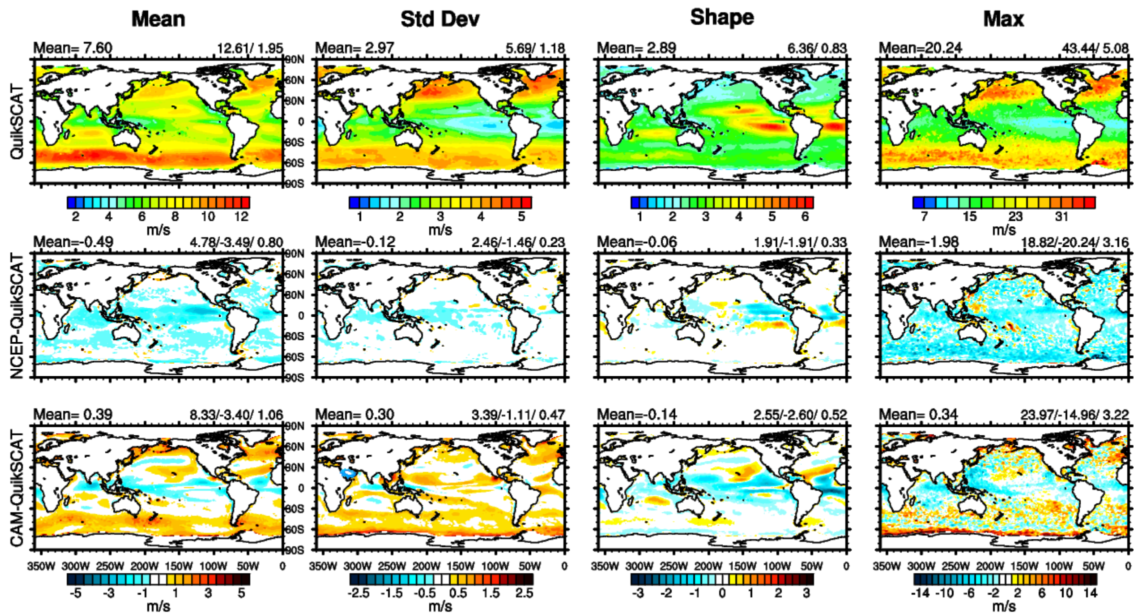

Figure 1: QuikSCAT 2000–2005 mean 10 m ocean surface wind speed, standard deviation, Weibull shape, and maximum (top row). NCEP−QuikSCAT differences and CAM3−QuikSCAT biases (rows two and three, respectively). Max/Min/RMSE values at each top right corner. CAM3 is sub-sampled at overflight times (Capps and Zender, 2007).

South and North America by $\sim 2.5\,\mathrm{m\,s^{-1}}$. The 6-year mean biases shown under-represent the root mean square bias in regions where errors of opposite signs mutually cancel when averaged.

I hypothesize that the non-linear dependence of surface momentum fluxes on wind speed (Figure 2) causes significant portions of these GCM wind speed biases. This would be consistent with previous studies concerned with the effects of surface flux non-linearities on air-sea exchange (e.g., Wang et al., 1998; Freely et al., 2004). This project will use QuikSCAT, TAO/TRITON and NCEP data to quantify and to remediate these biases. Surface energy and momentum fluxes are usually estimated as a function of mean wind speed, stability, and thermodynamic gradients based on extensive *in-situ* studies (e.g., Edson et al., 2007; Miller et al., 1992; Fairall et al., 1996). When all other properties are held constant, stronger ocean surface winds drive strongly non-linear momentum fluxes. The non-linearity is convex, such that momentum fluxes increase more per unit wind speed as wind speed increases (Renfrew et al., 2002)(Figure 2). The convex shape of the surface drag response to stronger winds dictates that the momentum flux predicted by the mean wind speed of a wind PDF is less than the mean momentum flux of the fully resolved wind PDF.

1.2 Surface Flux Biases

Typically GCMs do not represent processes on scales smaller than 100 km, such as mesoscale circulations, thermal and mechanically-induced turbulence, and convective downdrafts. Because of their non-linearity with wind speed, surface fluxes strongly depend on these sub-grid scale sources of wind variability which contribute significantly to the mean climate state. Mesoscale enhancement of surface fluxes resulting from sub-gridscale convection accounts for up to 30% of total tropical ocean fluxes (Esbensen and McPhaden, 1996). Miller et al. (1992) improved simulated tropical circulation and precipitation distribution by accounting for convectively-induced wind variability. Negatively buoyant downdrafts from precipitating cumulonimbus clouds also create sub-grid fluctuations in surface winds. Often, the spatial extent of these downdrafts is much greater than the convective cloud itself (Johnson and Nicholls, 1983).

2. APPROACH

My approach to capturing the influence of subgridscale winds on climate is to parameterize

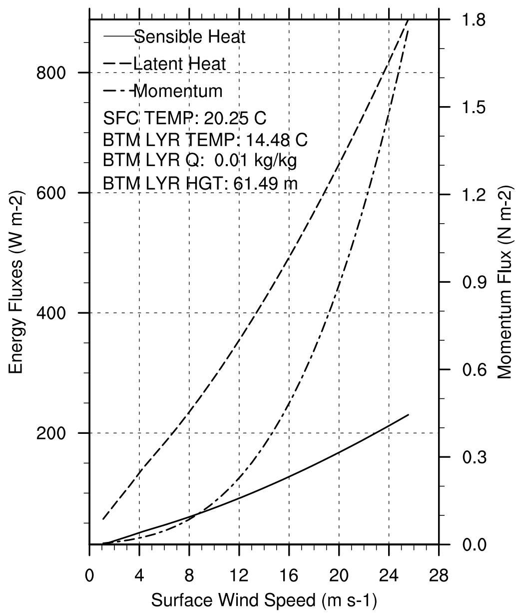

Figure 2: Ocean surface energy and momentum flux dependence on wind speed from Fairall et al. (1996) as used in CAM3.

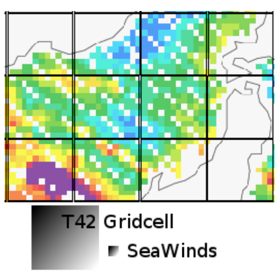

Figure 3: Instantaneous QuikSCAT wind vector observations at $0.25^\circ \times 0.25^\circ$ plotted over a T42-resolution grid (dark lines). Colors denote wind speed ranging from $1\,\mathrm{m\,s^{-1}}$ (blue) to $15\,\mathrm{m\,s^{-1}}$ (purple).

the physical information present in the QuikSCAT dataset which, at $0.25^\circ \times 0.25^\circ$ spatial resolution, has areal resolution $\mathcal{O}(100)$ times finer than typical GCMs (Figure 3). The (approximately 160) sub-gridscale QuikSCAT data points define the observed spatial and temporal wind speed PDF in each typical T42 GCM grid cell. QuikSCAT captures (twice per day) the remarkable spatial variation of sub-gridscale winds (Figure 3).

2.1 Quantifying Variability

I fit the observed and modeled wind distributions to the two-parameter Weibull PDF which has long been used for surface wind speeds (e.g., Justus et al., 1979; Monahan, 2006b). The Weibull scale and shape parameters characterize the mean wind speed and wind variability, respectively. The shape parameter $k \approx (\bar{U}/\sigma)^{1.086}$ varies nearly linearly with mean wind speed $\bar{U}$ and inversely with the standard deviation σ. Regions with moderate and persistent mean wind speeds (trade-winds) have moderate shape values (~ 8) while regions with low mean winds and high variability (the doldrums) have shape values near 2 (Figure 1, third column).

CAM overestimates the persistence of the trades and overestimates gustiness within the doldrums. Positive shape biases up to 1.5 occur in the trade-wind region northwest of Australia and the north Atlantic and Pacific trades. Large negative biases $\sim 50\%$ of observed shape values are found throughout the equatorial regions. Regions where the measured and modeled mean winds agree and the shape values (i.e., PDF breadth) do not are particularly interesting. My premise is that within these regions CAM3 surface flux biases can be remediated by redistributing the predicted PDF (which has the correct mean wind speed) into the observed PDF.

2.2 Sensitivity to Sub-gridscale Winds

I tested the sensitivity of modeled surface fluxes to representation of the sub-gridscale wind PDF to ascertain the approximate magnitude of the flux bias attributable to completely neglecting sub-gridscale winds. In this study, CAM is forced with observed SSTs from 2000–2005, coincident with the QuikSCAT period. At each 20-minute timestep, CAM calculated two different sets of surface fluxes: (1) The control, based on gridcell mean wind speed $\bar{U}$, and (2) The experiment, which resolves a four bin wind speed PDF which preserves $\bar{U}$ and diagnoses the PDF width from $\bar{U}$ based on empirical studies of Justus et al. (1978).

The sensitivity, illustrated by the difference (experiment$-$control) in the mean June results (Figure 4), is largest for the momentum fluxes. This is not unexpected, since momentum is most non-linear with wind speed (cf. Figure 2). The experiment (resolved sub-gridscale PDF) dissipates $\sim 0.02\,\mathrm{N\,m^{-2}}$ (about 10%) more momentum than the control in the June global mean (Figure 4). This is most pronounced in the southern ocean, where winds are strong. The sub-grid winds change the climatological June latent and sensible heat fluxes by only $\sim 1\%$ on average. Sensitivities of

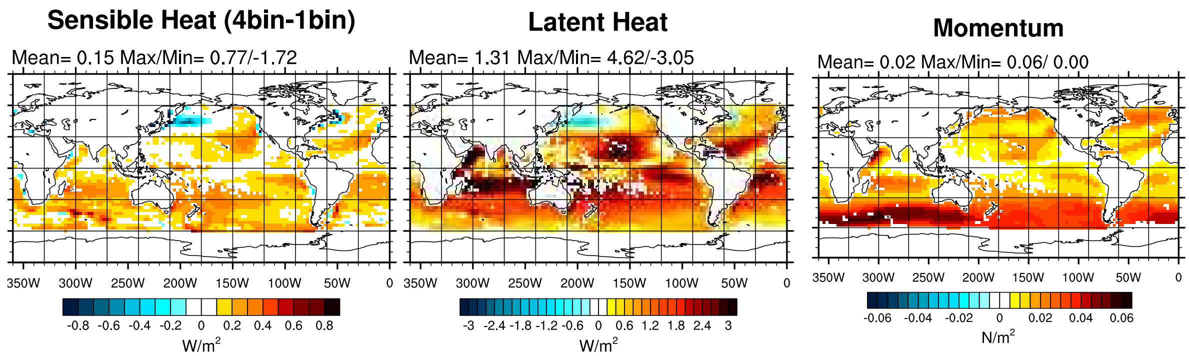

Figure 4: Sensitivity of mean 2000–2005 June sensible heat (left), latent heat (middle) and momentum (right) fluxes to representation of sub-gridscale winds. Differences show predictions with four wind bins per gridcell minus standard one-bin predictions.

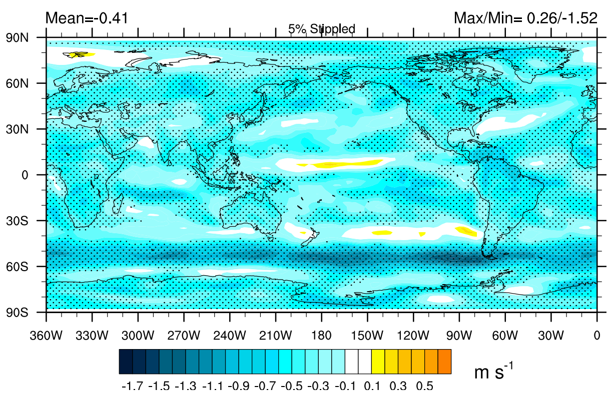

Figure 5: Changes in near surface wind speed when resolving a 4-bin wind PDF compared to a single gridcell mean wind speed (10-year T42 CAM3 simulations).

the energy fluxes have pronounced regional and seasonal structure near western boundary currents (due to strong air-sea temperature contrasts) and in the subtropics (probably due to strong surface insolation/evaporation).

In a similar study, a 4-bin non-physical wind speed PDF was implemented within CAM forced by a slab ocean model. The 10-year duration of this simulation provided ample time to allow for changes in surface flux climatologies to feedback throughout the climate. The results of this simulation suggest that the non-linear momentum flux response to sub-gridscale winds results in a reduction in GCM mean wind speed biases (Figure 5). Especially encouraging is the reduction in mean wind speed throughout the trades and SH circumpolar.

2.3 Determining Physically Based Wind PDFs

I will combine QuikSCAT-observed wind PDFs with TAO/TRITON and NCEP-estimated atmospheric states to diagnose physically-based surface sub-gridscale wind PDFs from the GCM-predicted atmospheric state. Following Cakmur et al. (2004), I will begin by assuming sub-gridscale winds originate primarily from three processes: thermally driven buoyancy, mechanically induced (shear-driven) turbulent kinetic energy (TKE), and convective downdrafts. Turbulence diagnostics utilized will include the Deardorff velocity (Deardorff, 1970), turbulence kinetic energy and downdraft mass flux. Each turbulence diagnostic will influence the shape parameter of the sub-gridscale wind PDF. These three processes are assumed to be uncorrelated, and to broaden the total PDF in quadrature.

4. BROADER SIGNIFICANCE

It is thought that climate change will increase weather extremes (Cubasch and Meehl, 2001) which often occur at the tail end of wind speed PDFs. Although several studies have analyzed the QuikSCAT global ocean surface wind climatology (Chelton and Freilich, 2005; Monahan, 2006a,b), ours is the first attempt (to our knowledge) to use QuikSCAT data to parameterize sub-gridscale winds for GCM predictions. Logically other GCMs that neglect sub-gridscale winds (all of them, to our knowledge) are susceptible to the biases described here. Moreover, the techniques I develop and apply to wind speed measurements could be modified to parameterize other sub-gridscale measurements (e.g., surface reflectance, canopy height, snow cover) into physical process models.

References

Bourassa, M. A., D. M. Legler, J. J. O'Brien and S. R. Smith, 2003: SeaWinds validation with research vessels. *J. Geophys. Res.*, **108**(C2), 3019.

Cakmur, R. V., R. L. Miller and O. Torres, 2004: Incorporating the effect of small-scale circulations upon dust emission in an atmopsheric general circulation model. *J. Geophys. Res.*, **109**(D07201).

Capps, S. B. and C. S. Zender, 2007: Characterization and comparison of sea surface wind speed distributions from QuikSCAT and CAM3. *Manuscript in preparation*, Available from http://dust.ess.uci.edu/ppr/ppr_CaZ07.pdf.

Chelton, D. B. and M. H. Freilich, 2005: Scatterometer-based assessment of 10-m wind analyses from the operational ECMWF and NCEP numerical weather prediction models. *Mon. Weather Rev.*, **133**, 409–429.

Collins, W. D., C. M. Bitz, M. L. Blackmon, G. B. Bonan, C. S. Bretherton, J. A. Carton, P. Chang, S. C. Doney, J. J. Hack, T. B. Henderson, J. T. Kiehl, W. G. Large and D. S. McKenna, 2006: The Community Climate System Model: CCSM3. *J. Climate*, **19**(11), 2122–2143.

Cubasch, U. and G. Meehl, 2001: Projections of future climate change. in *Climate Change 2001: The Scientific Basis. Contribution of Working Group I to the Third Assessment Report of the Intergovernmental Panel on Climate Change*, Chap. 9, pp. 527–578. Cambridge Univ. Press, Cambridge, UK, and New York, NY, USA.

Deardorff, J. W., 1970: Convective Velocity and Temperature Scales for the Unstable Planetary Boundary Layer and for Rayleigh Convection. *J. of the Atmospheric Sciences*, **27**, 1211–1213.

Donelan, M., W. Drennan, E. Saltzman and R. Wanninkhof, 2002: *Gas Transfer at Water Surfaces*. American Geophysical Union, Washington D. C.

Edson, J., T. Crawford, J. Crescenti, T. Farrar, N. Frew, G. Gerbi, C. Helmis, T. Hristov, D. Khelif, A. Jessup, H. Jonsson, M. Li, L. Mahrt, W. McGillis, A. Plueddemann, L. Shen, E. Skyllingstad, T. Stanton, P. Sullivan, J. Sun, J. Trowbridge, D. Vickers, S. Wang, Q. Wang, R. Weller, J. Wilkin, A. J. Williams, III, D. K. P. Yue and C. Zappa, 2007: The coupled boundary layers and air-sea transfer experiment in low winds. *Bull. Am. Meteorol. Soc.*, **88**(3), 341–356.

Esbensen, S. K. and M. J. McPhaden, 1996: Enhancement of tropical ocean evaporation and sensible heat flux by atmospheric mesoscale systems. *J. Climate*, **9**(10), 2307–2325.

Fairall, C. W., E. F. Bradley, D. P. Rogers, J. B. Edson and G. S. Young, 1996: Bulk parameterization of air-sea fluxes for Tropical Ocean-Global Atmosphere Coupled-Ocean Atmosphere Response Experiment. *J. Geophys. Res.*, **101**(C2), 3747–3763.

Freely, R. A., R. Wanninkhof, W. McGillis, M.-E. Carr and C. E. Cosca, 2004: Effects of wind speed and gas exchange parameterizations on air-sea CO_2 fluxes in the equatorial Pacific Ocean. *J. Geophys. Res.*, **109**(C08S03).

Johnson, R. H. and M. E. Nicholls, 1983: A composite analysis of the boundary layer accompanying a tropical squall line. *Mon. Weather Rev.*, **111**(2), 308–319.

Justus, C. G., W. R. Hargraves, A. Mikhail and D. Graber, 1978: Methods for estimating wind speed frequency distributions. *J. Appl. Meteorol.*, **17**, 350–353.

Justus, C. G., K. Mani and A. S. Mikhail, 1979: Interannual and month-to-month variations of wind speed. *J. Appl. Meteorol.*, **18**, 913–920.

Miller, M. J., A. C. M. Beljaars and T. N. Palmer, 1992: The sensitivity of the ECMWF model to the parameterization of evaporation from the tropical oceans. *J. Climate*, **5**, 418–434.

Monahan, A. H., 2006a: The probability distribution of sea surface wind speeds. Part I: Theory and seawinds observations. *J. Climate*, **19**, 497–520.

Monahan, A. H., 2006b: The probability distribution of sea surface wind speeds. Part II: Dataset intercomparison and seasonal variability. *J. Climate*, **19**, 521–534.

Renfrew, I. A., G. W. K. Moore, P. S. Guest and K. Bumke, 2002: A comparison of surface layer and surface turbulent flux observations over the labrador sea with ECMWF analyses and NCEP reanalyses. *J. Phys. Oceanography*, **32**, 383–400.

Wang, C., R. H. Weisberg and H. Yang, 1998: Effects of the wind speed-evaporation-SST feedback on the El Niño-Southern Oscillation. *J. Atmos. Sci.*, **56**(10), 1391–1403.

Weller, R. A. and S. P. Anderson, 1996: Surface meteorology and air-sea fluxes in the western equatorial pacific warm pool during the TOGA coupled ocean-atmosphere response experiment. *J. Climate*, **9**, 1959–1990.